Photophysical and Nonlinear Optical Properties of [60]Fullerene Derivatives†

Ya-Ping Sun,* Glenn E. Lawson, Jason E. Riggs, Bin Ma, Naixing Wang, and Dwella K. Moton

Department of Chemistry, Howard L. Hunter Chemistry Laboratory, Clemson University, Clemson, South Carolina 29634-1905

Received: November 6, 1997; In Final Form: February 3, 1998

A systematic spectroscopic study of a series of C_{60} derivatives with different cage functionalizations is reported. The absorption spectra and absorptivities of the derivatives in solution were measured and compared. By recording the fluorescence spectra using a near-infrared-sensitive emission spectrometer (extending to 1200 nm), fluorescence quantum yields of the derivatives were determined quantitatively. Fluorescence lifetimes of the derivatives were obtained using the time-correlated single photon counting technique. The results show that both fluorescence quantum yields and lifetimes are rather similar for the different classes of C_{60} derivatives. The nonlinear absorptive properties of the derivatives were evaluated by optical limiting measurements in solution and in polymer film using the second harmonic of a Q-switched Nd:Yag laser at 532 nm. Effects of different fullerene cage functionalizations on the photophysical properties and optical limiting responses of the C_{60} derivatives are discussed.

Introduction

The electronic transitions and excited state properties of fullerenes, especially [60]fullerene (C_{60}), have attracted much attention.[1,2] It is now well established that the low-lying electronic transitions in C_{60} are only weakly allowed because of the high degree of symmetry in the closed-shell electronic configuration. The absorption band of C_{60} in the visible is very weak, with the molar absorptivity at the band maximum of only $\sim$950 $M^{-1}cm^{-1}$.[3−5] In fact, only a small fraction of the broad visible absorption band in the 430 $\sim$ 670 nm region is due to the contribution of the transition to the lowest excited singlet state.[6] Upon photoexcitation, the excited singlet state decays are dominated by intersystem crossing to the excited triplet state. As a result, C_{60} is only weakly fluorescent, with a very low fluorescence quantum yield of 3.2×10^{-4} in room-temperature toluene.[6] The extremely efficient intersystem crossing produces a high population of the excited triplet state. Because of higher triplet−triplet transient absorption cross sections than the ground-state absorption cross sections,[7,8] C_{60} is an excellent broad-band nonlinear absorber for potential optical limiting and optical switching applications.[9−24]

With a large number of methods developed for functionalizing the fullerene cage,[25,26] various C_{60} derivatives have recently been studied for an understanding of the effects of derivatization on the photophysical properties of C_{60}.[27−30] Among the compounds under active investigations are methano-C_{60} and pyrrolidino-C_{60} derivatives, which represent two important classes of functionalized fullerene molecules.[25,26,31,32] It has been shown[30] that the photophysical properties of methano-C_{60} and pyrrolidino-C_{60} derivatives are somewhat different from those of C_{60}. The derivatives have higher ground-state absorptivities than C_{60} due largely to a reduction in molecular symmetry. The increases in transition probability are also reflected in the larger fluorescence radiative rate constants of the derivatives. As a result, from C_{60} to the derivatives, the increases in the fluorescence quantum yields are larger than those in the fluorescence lifetimes. Particularly interesting is the fact that the methano-C_{60} derivatives with very different functional groups on the methano bridge exhibit essentially the same photophysical behavior.[30] In addition, the nonlinear absorptive properties of the C_{60} derivatives as measured by their optical limiting responses toward a nanosecond pulsed laser at 532 nm are similar to that of C_{60}.[24] However, C_{60} derivatives have more favorable solubility characteristics, which are advantageous in the fabrication of the nonlinear absorptive materials into optical devices.

In this paper, we report a systematic spectroscopic study of a series of C_{60} derivatives with different cage functionalizations. The absorption spectra and absorptivities of the derivatives in solution were measured and compared. By recording the fluorescence spectra using a near-infrared (IR)-sensitive emission spectrometer (extending to 1200 nm), fluorescence quantum yields of the derivatives were determined quantitatively. Fluorescence lifetimes of the derivatives were obtained by the time-correlated single photon counting technique. The results show that both fluorescence quantum yields and lifetimes are rather similar for the different classes of C_{60} derivatives. The nonlinear absorptive properties of the derivatives were evaluated by optical limiting measurements in solution and in polymer film using the second harmonic of a Q-switched Nd:Yag laser at 532 nm. Effects of different fullerene cage functionalizations on the photophysical properties and optical limiting responses of the C_{60} derivatives are discussed.

Experimental Section

Materials. C_{60} (purity >99.5%) was obtained from Bucky-USA and was used without further purification. All solvents are of spectrophotometry grade. Because no interference of possible impurities in the wavelength range of interest was found in absorption and emission spectroscopic measurements, the solvents were used as received.

Methano-C_{60} Derivatives I−III. The methano-C_{60} derivative **I** was prepared by the reaction of C_{60} with the stabilized sulfonium ylide.[30,33] The one-pot preparation was carried out

† This paper is dedicated to Professor Jack Saltiel on the occasion of his 60th birthday.

S1089-5639(98)00112-1 CCC: $15.00
Published on Web 03/26/1998

under phase transfer condition. A solution of 500 mg of C_{60} (0.69 mmol) in 500 mL of anhydrous toluene, 220 mg of sulfonium bromide (1.2 mmol), 1 g of anhydrous K_2CO_3 (7.1 mmol), and 50 mg of the phase transfer catalyst tetrabutylammonium bromide (TBAB, 0.155 mmol) were mixed in a 1-L round-bottomed flask. After purging with dry nitrogen gas, the flask was sealed and the reaction mixture was stirred at room temperature for 24 h. The stabilized sulfonium ylide generated in situ due to the deprotonation of the sulfonium salt by K_2CO_3 under the catalysis of TBAB undergoes nucleophilic addition to C_{60}, followed by intramolecular substitution to form the methano-C_{60} derivative **I** with the simultaneous elimination of dimethyl sulfide. The reaction mixture was filtered to remove any solids and then concentrated by evaporation under reduced pressure. The matrix-assisted laser desorption ionization time-of-flight MS analysis shows the presence of mono-, bis-, and tris-adducts. The monoadduct was obtained after separation from higher order adducts through silica gel column chromatography using toluene as an eluent. The yield for the methano-C_{60} derivative **I** is ~50%. Proton and ^{13}C NMR results clearly show that the methylene bridge is at the [6,6]-ring junction.

The methano-C_{60} derivative **II** was obtained from the hydrolysis of **I**.[31] In the preparation, 350 mg of **I** (0.42 mmol) and 151 mg of 4-toluenesulfonic acid (0.795 mmol) in 275 mL toluene were refluxed for ~8 h. Then, 275 mL water was added, and the mixture was stirred for 30 min. The water layer was decanted, and the toluene layer was filtered to yield a brown solid. The solid sample was washed with water and ethanol and then dried for ~12 h at 60 °C, yielding 185 mg of the derivative **II** (57% yield).

The methano-C_{60} derivative **III** was prepared in the coupling reaction of **II** with diethylamine (DEA) using 1-ethyl-3-(dimethylaminopropyl)carbodimide (EDAC) as a coupling agent.[34] In the preparation, a mixture of 20 mg of **II**, 6 μL of DEA, 6 μL of triethylamine, and 9.2 mg of EDAC in 6 mL of bromobenzene was stirred for ~20 h. The reaction mixture was separated on a silica gel column using chloroform as an eluent, yielding 10 mg of the derivative **III** (47% yield).

Methano-C_{60} Derivatives IV and V. The methano-C_{60} derivative **IV** was prepared following a procedure reported in the literature,[35] except that a lower molar ratio of bromomalonate to C_{60} (1.2:1) was used to promote the formation of monoadduct. In the reaction, nucleophilic addition of bromomalonate carbanion from the deprotonation of bromomalonate with sodium hydride was followed by intramolecular substitution.[35] The reaction mixture consists of mono-, bis-, and trisadducts. The monoadduct was separated from the mixture in 55% yield by silica gel column chromatography using toluene as an eluent. The derivative **V** was obtained from the hydrogenolysis of **IV** by a procedure reported in the literature.[36]

C_{60} Derivative VI. The C_{60} derivative **VI** was obtained as a byproduct in the photochemical reaction of C_{60} with triethylamine in an air-saturated toluene solution.[37] The purification and structural characterization of the compound will be reported separately.

Amino-C_{60} Derivative VII. The amino-C_{60} derivative **VII** was prepared in the photochemical reaction of C_{60} with *N,N′*-dimethyl-1,2-ethylenediamine. The photoirradiation was carried out by use of an ACE Glass ACE−7861 type immersion-well photochemical reaction assembly equipped with a 450-W Hanovia medium-pressure mercury lamp. A solution of 518 mg (5.9 mmol) of *N,N′*-dimethyl-1,2-ethylenediamine in 40 mL of toluene was added in a dropwise manner with stirring to a solution of 580 mg (0.81 mmol) of C_{60} in 260 mL of toluene in the reaction vessel. The solution mixture was purged with dry nitrogen gas for ~1 h before photoirradiation, and the loss of solvent during the nitrogen purging was prevented by attaching a condenser to the outlet of the reaction vessel. An aqueous solution of potassium chromate (0.1 g/mL) was used as a liquid cutoff filter (505 nm). The photoirradiation was for 70 min under nitrogen atmosphere. The solution was then put on a rota-vap to remove the solvent toluene. The solid reaction mixture was extracted repeatedly using CS_2. The CS_2 solution was then concentrated and separated on a silica gel column using hexane−50% (v/v) toluene, methylene chloride, and then methylene chloride −0.8% (v/v) methanol as eluents, yielding 150 mg of the amino-C_{60} derivative **VII** (23% yield). The compound was positively identified in matrix-assisted laser desorption ionization time-of-flight MS and proton and ^{13}C NMR characterizations.[38]

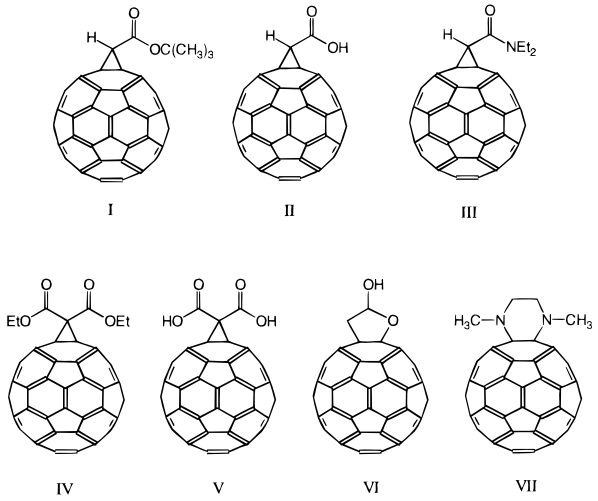

Measurements. Absorption spectra were obtained using a computer-controlled Shimadzu UV2101−PC spectrophotometer. Emission spectra were recorded on a Spex Fluorolog-2 photon-counting emission spectrometer equipped with a 450-W xenon source, a Spex 340S dual-grating and dual-exit emission monochromator, and two detectors. The two gratings are blazed at 500 nm (1200 grooves/mm) and 1000 nm (600 grooves/mm). The room-temperature detector consists of a Hamamatsu R928P photomultiplier tube operated at −950 V, and the thermoelectrically cooled detector consists of a near-IR-sensitive Hamamatsu R5108 photomultiplier tube operated at −1500 V. In fluorescence measurements, a Schott 540 nm (GG-540) or 610 nm (RG-610) color glass sharp-cut filter was placed before the emission monochromator to eliminate the excitation scattering. Minor distortion at the blue onset of the observed fluorescence spectra due to the filter was corrected by use of the transmittance profile of the filter. The slit of the excitation monochromator was 5 mm (19 nm resolution). For the emission monochromator, a wide slit of 5 mm (19 nm resolution) was used in fluorescence quantum yield measurements to reduce experimental uncertainties, and a narrow slit of 0.5 mm (2 nm resolution) was used in fluorescence spectral measurements to retain structures of the spectra. Unless otherwise specified, fluorescence spectra were corrected for nonlinear instrumental response with predetermined correction factors. The correction factors for the emission spectrometer were carefully determined with a calibrated radiation standard from Optronic Laboratories.

Fluorescence decays were measured by the time-correlated single photon counting (TCSPC) method. The TCSPC setup consists of a Hamamatsu Stabilized Picosecond Light Pulser

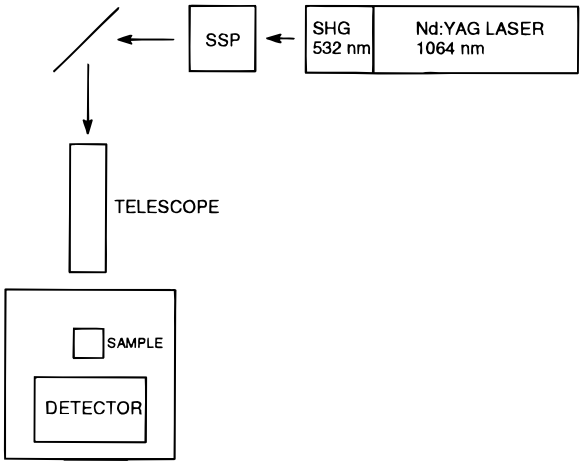

Figure 1. Experimental setup for optical limiting measurements.

(PLP-02) as the excitation source, which produces ~33 ps (fwhm) light pulses at 632-nm with a repetition rate of 1 MHz. Fluorescence decays were monitored through a 695-nm color glass sharp-cut filter. The detector consists of a Hamamatsu R928P photomultiplier tube operated at −1 kV using an EG&G Ortec 556 high-voltage power supply. The detector electronics from EG&G Ortec include two 9307 discriminators, a 457 biased time-to-amplitude converter, and a 916A multichannel analyzer. The instrument response function of the setup has a fwhm of ~2.5 ns. Fluorescence lifetimes were determined from observed decay curves and instrument response functions through deconvolution by the Marquardt nonlinear least-squares method.

Optical limiting measurements were performed with the setup illustrated in Figure 1. This setup consists of a Continuum Surelite-I Q-switched Nd:YAG laser as the light source, which can be operated from a single shot to 10 Hz. The IR fundamental was frequency doubled to generate the second harmonic at 532 nm which was isolated with a Surelite harmonic separation package. The maximum energy at 532 nm is 160 mJ/pulse, with a 5-ns pulse width (fwhm). The laser output was varied in a range 10−160 mJ/pulse with a waveplate-polarizer combination. The laser beam has a diameter of 6 mm, corresponding to energy densities 0.035−0.57 J/cm^2. A Galilean style telescope consisting of a plano-concave lens and a plano-convex lens was used to reduce the laser beam waist to 3 mm in diameter for higher energy densities up to 2.2 J/cm^2. A Scientech Mentor MC2501 calorimeter and a MD10 m were used as the detector. Solution samples were measured in a cuvette with 2 mm optical path length.

Results

UV−Vis Absorption. UV−vis absorption spectra of the C_{60} derivatives were measured in room-temperature (22 °C) solutions. The spectra of the methano-C_{60} derivatives shown in Figure 2 are similar to those of other methano-C_{60} derivatives reported previously.[25−31] For the C_{60} derivative **VI**, the absorption spectrum is more similar to those of pyrrolidino-C_{60} derivatives.[30,32] However, the absorption spectrum of the amino-C_{60} derivative **VII** is noticeably different. Although it has a shoulder at ~695 nm, as in other monofunctionalized C_{60} derivatives, the sharp peak at 400−450 nm as a common feature in the spectra of methano- and pyrrolidino-C_{60} derivatives and the derivative **VI** is absent. The similarities and differences between the absorption spectra of different classes of C_{60} derivatives are easily recognized in a direct comparison shown in Figure 3. An interesting observation is that although the absorption spectral profiles of different classes of C_{60} derivatives are somewhat different, their absorptivities in the visible region are rather similar.

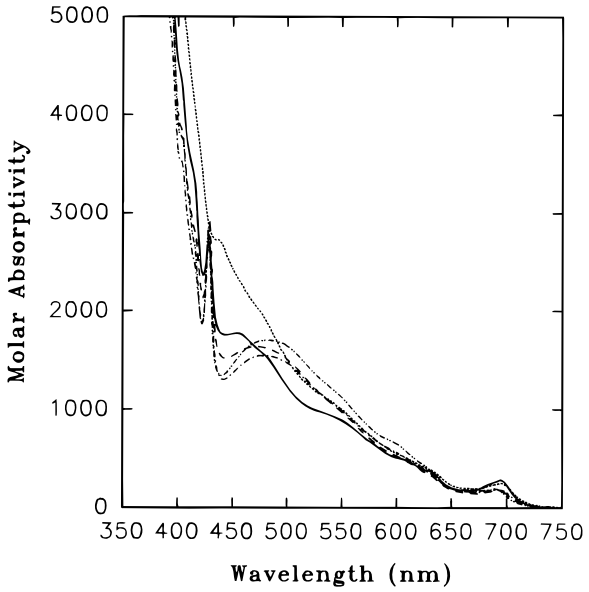

Figure 2. Absorption spectra of the methano-C_{60} derivatives **II** (-·-·-), **III** (- - -), and **V** (-···-···-), the C_{60} derivative **VI** (—), and the amino-C_{60} derivative **VII** (···) in room-temperature solutions (Table 1).

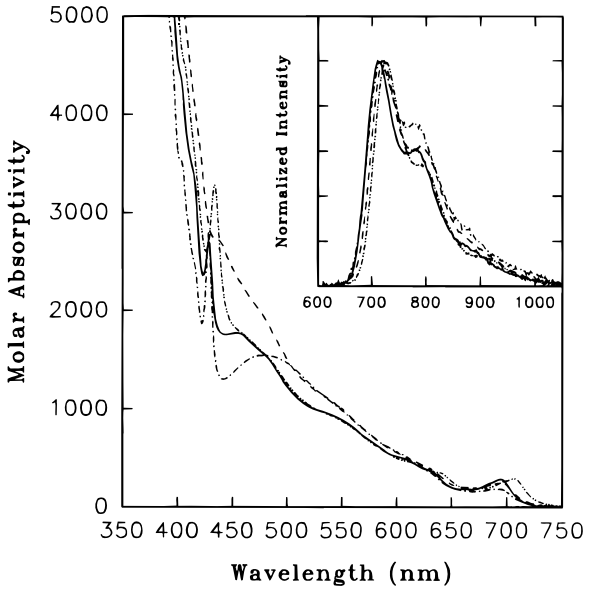

Figure 3. A comparison of the absorption and fluorescence (inset) spectra of different classes of C_{60} derivatives: the methano-C_{60} derivative **II** (-·-·-), the pyrrolidino-C_{60} derivative *N*-ethyl-*trans*-2′,5′-dimethylpyrrolidino[3′,4′:1,2]C_{60} (-···-···-),[30] the C_{60} derivative **VI** (—), and the amino-C_{60} derivative **VII** (- - -).

Fluorescence Spectra. Fluorescence spectra of the C_{60} derivatives in room-temperature solutions were measured with an emission spectrometer that is sensitive in the near-IR region (up to 1200 nm). As shown in Figure 4, the spectra of the different derivatives have similar features, with a peak at 690−695 nm and two shoulders at longer wavelengths. Shown in the inset of Figure 3 is a more direct comparison of the different classes of C_{60} derivatives. The relative intensities of the peak and shoulders in the fluorescence spectra of the derivative **VI** and the amino-C_{60} derivative **VII** are quite similar.

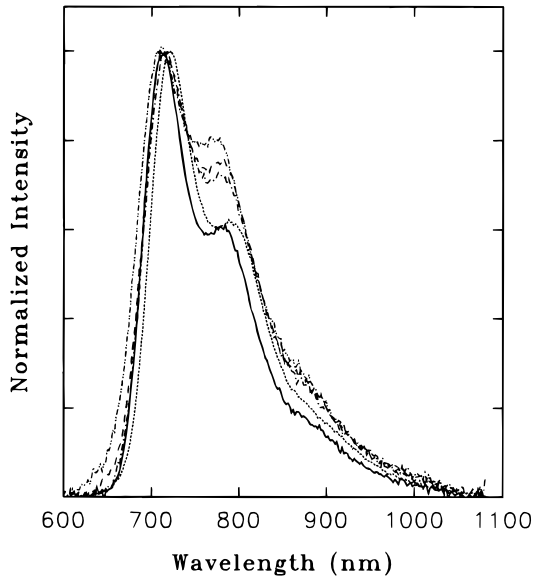

Figure 4. Fluorescence spectra of the methano-C_{60} derivatives **II** (-·-·-), **III** (- - -), and **V** (-···-··-), the C_{60} derivative **VI** (—), and the amino-C_{60} derivative **VII** (···) in room-temperature solutions (Table 1).

TABLE 1: Photophysical Properties of the C_{60} Derivatives

compound	solvent	ABS_{0-0} (nm)	ϵ_{0-0} (M^{-1} cm^{-1})	$FLSC_{0-0}$	Φ_F (10^{-3})	τ_F (ns)
C_{60}	toluene				0.32	1.2
I	toluene	692	190	713	1.0	1.49
II	THF	694	185	716	0.8	1.46
III	$CHCl_3$	692	176	713	0.99	1.45
IV	$CHCl_3$	688	195	715	1.0	1.48
V	THF	690		715		
VI	$CHCl_3$	694	283	712	0.93	1.6
VII	toluene	694	150	713	0.91	1.3

Fluorescence Quantum Yields. Fluorescence quantum yields of the C_{60} derivatives in room-temperature solutions were determined quantitatively in reference to the yield of C_{60} (3.2×10^{-4}), which was obtained using rhodamine 101 in ethanol as a fluorescence standard ($\Phi_F = 1.0$).[6] Because different solvents were used because of solubility considerations, the results of experimental measurements were corrected for effects due to changes in solvent refractive index n.[39]

$$\Phi_F = \Phi_F'(n/n_{SD})^{-2} \quad (1)$$

where SD represents the solvent for the standard from which the uncorrected fluorescence yield value Φ_F' is obtained. The C_{60} derivatives are apparently more fluorescent than the parent C_{60}, with the yields of the derivatives being ~3 times higher than that of C_{60} (Table 1). However, despite different molecular structures of the C_{60} derivatives, their fluorescence yields are rather similar, varying in a narrow range of 8×10^{-4} to 1×10^{-3} (Table 1). The observed fluorescence quantum yields of the C_{60} derivatives are excitation wavelength independent.

Fluorescence Lifetimes. Fluorescence decays of the C_{60} derivatives in room-temperature solutions were measured by the TCSPC method. The result for the derivative **VI** is shown in Figure 5 as an example. The decays can be deconvoluted well from corresponding instrumental response functions using a monoexponential equation. The fluorescence lifetimes of the C_{60} derivatives are somewhat longer than that of C_{60}, varying in a range of 1.3 to 1.6 ns (Table 1).

Optical Limiting. The optical limiting properties of the C_{60} derivatives in room-temperature solutions were measured with the setup shown in Figure 1. For the methano-C_{60} derivatives **I**−**V**, optical limiting responses were compared by using solutions with linear transmittances of 55 and 70% at 532 nm. The solutions show significant optical limiting, with a nonlinear relationship between the output (I_{OUT}) and input (I_{IN}) light fluences (Figure 6). At high input fluences, I_{OUT} reaches a plateau. For the C_{60} derivative **III**, as an example, the saturated

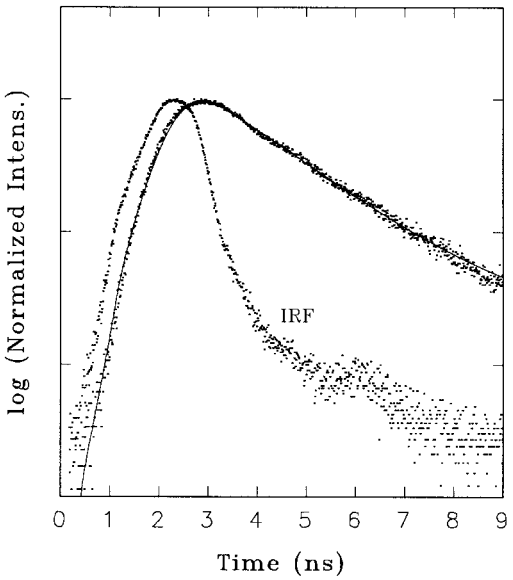

Figure 5. The fluorescence decay of the C_{60} derivative **VI** in room-temperature toluene. The solid line is from least-squares fit.

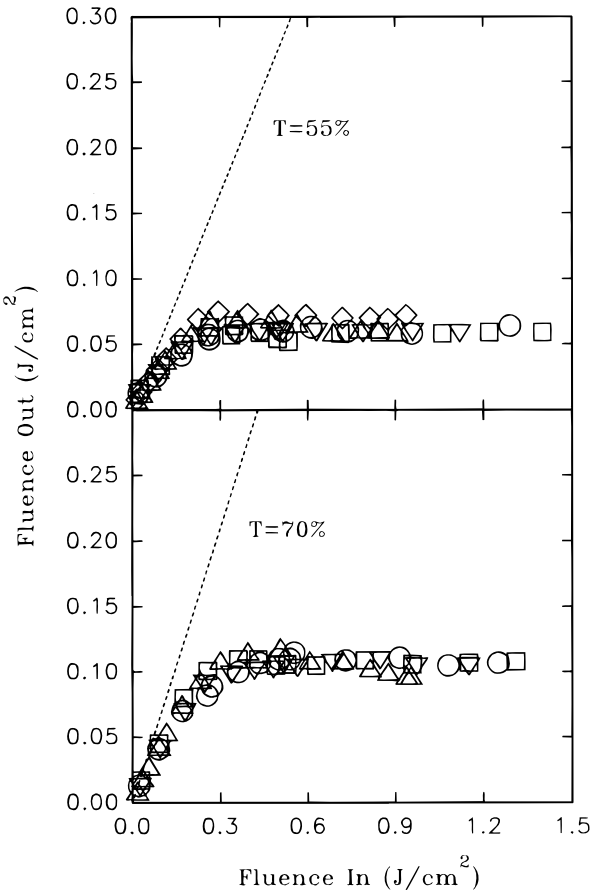

Figure 6. Optical limiting results of the methano-C_{60} derivatives **I** in chloroform (○), **II** in chloroform − 10% v/v DMSO (▽), **III** in chloroform (□), **IV** in chloroform (△), and **V** in THF (◇) solutions with 55 and 70% linear transmittances at 532 nm.

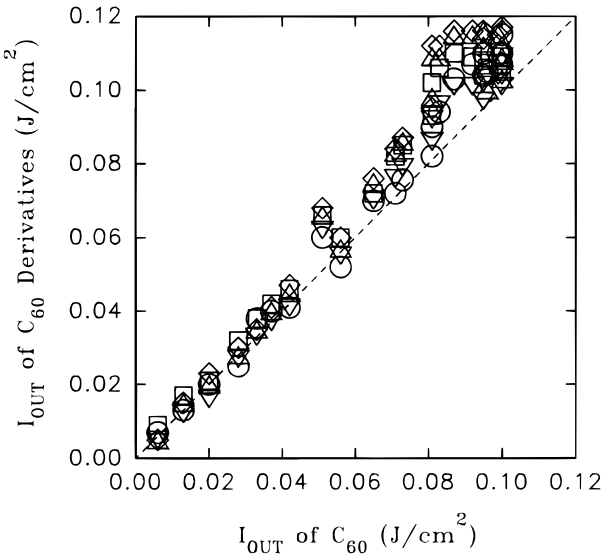

Figure 7. Plots of the output light fluences for the methano-C_{60} derivatives **I** (○), **II** (▽), **III** (□), **IV** (△), and **V** (◇) versus those for C_{60} at the same input light fluences and the same linear transmittance of 70% at 532 nm.

TABLE 2: Optical Limiting Properties of the C_{60} Derivatives

		I_{OUT} at saturation (J/cm^2)		
sample	solvent	$T = 55\%$	$T = 70\%$	$T = 72\%$
C_{60}	toluene	0.05_5	0.1	0.12
I	$CHCl_3$	0.06	0.11	
II	$CHCl_3$ + 10%DMSO	0.06	0.11	
III	$CHCl_3$	0.06	0.11	
IV	$CHCl_3$	0.06	0.1	
V	THF	0.07	0.12	
VI	toluene			0.12_5
VII	toluene	0.06		0.13

I_{OUT} values at the plateau are ~0.06 and ~0.11 J/cm^2 for the solutions of 55 and 70% linear transmittances, respectively. A comparison of the saturated I_{OUT} values for the different methano-C_{60} derivatives in room-temperature solutions is shown in Table 2. The optical limiting responses of the methano-C_{60} derivatives are quite similar to those of C_{60} in toluene. For a more direct comparison, shown in Figure 7 are plots for the I_{OUT} values of the methano-C_{60} derivatives vs the I_{OUT} values of C_{60} at the same input fluences. The plots are close to linear, with slopes near unity, indicating that the nonlinear absorptions in the methano-C_{60} derivatives and in C_{60} are essentially the same.

The optical limiting responses of the C_{60} derivative **VI** in room-temperature toluene solution with a linear transmittance of 72% were determined. As shown in Figure 8, the I_{OUT} is also strongly nonlinear with respect to I_{IN}, reaching a plateau at the input fluence of ~0.3 J/cm^2. The saturated I_{OUT} value at the plateau is ~0.125 J/cm^2, which is essentially the same as that of C_{60} in toluene solution. A direct comparison of I_{OUT} values of the derivative **VI** and C_{60} at the same I_{IN} values is shown in Figure 9. The plot is close to the 45° line, which shows again that the optical limiting responses of the derivative **VI** are similar to those of C_{60}.

The amino-C_{60} derivative **VII** exhibits similar optical limiting responses (Figure 10). For **VII** in room-temperature toluene with linear transmittances of 55 and 72% at 532 nm, the output fluences reach saturation at input fluences of ~0.2 and ~0.3 J/cm^2, respectively, with the saturated I_{OUT} values of ~0.06 and ~0.13 J/cm^2 for the solutions of 55 and 72% linear transmittances, respectively. Shown in Figure 9 is again a more direct comparison of the optical limiting responses between C_{60} and the amino-C_{60} derivative **VII** at the linear transmittance of 72%, where the I_{OUT} values of **VII** are plotted against the I_{OUT} values of C_{60} at the same input fluences. This plot is also close to the 45° line.

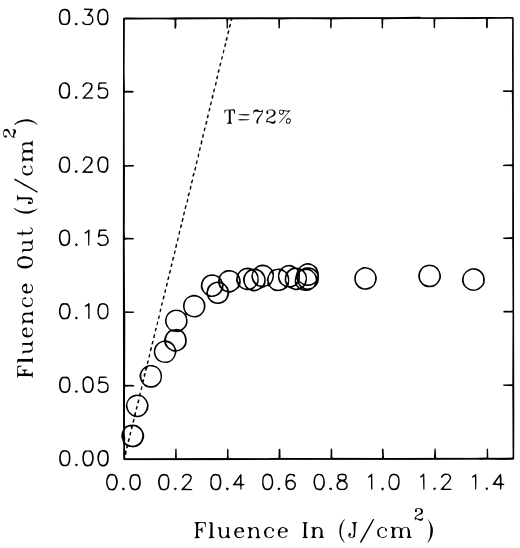

Figure 8. Optical limiting responses of the C_{60} derivative **VI** in toluene solution of 72% linear transmittance at 532 nm.

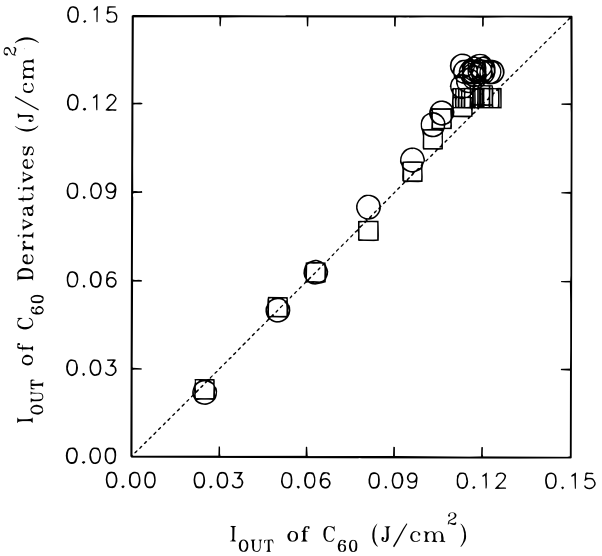

Figure 9. Plots of the output light fluences for the C_{60} derivatives **VI** (□) and **VII** (○) versus those for C_{60} at the same input light fluences and the same linear transmittance of 72% at 532 nm.

A systematic comparison for the optical limiting responses of C_{60} and the C_{60} derivatives in room-temperature solutions with similar linear transmittances at 532 nm is shown in Table 2.

Optical limiting measurements were also carried out for the methano-C_{60} derivative **I** incorporated in polymethyl methacrylate (PMMA) films. The films of ~0.4 mm thickness were prepared by solution casting. In the preparation, a viscous toluene solution of the C_{60} derivative **I** and PMMA polymer (M_W ~ 315 000) was added to a glass mold to allow a slow evaporation of the solvent toluene. The film samples were then allowed to cure for several days to ensure a complete removal of the solvent. The linear transmittance of the films was varied by adjusting the concentration of the C_{60} derivative **I** in the

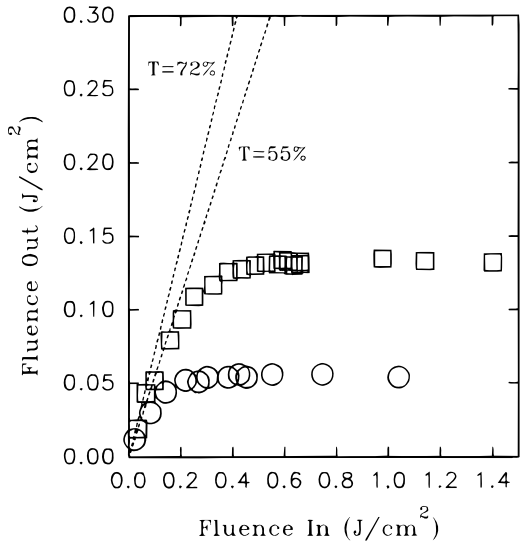

Figure 10. Optical limiting results of the amino-C_{60} derivative **VII** in toluene solutions with 55% (○) and 72% (□) linear transmittances at 532 nm.

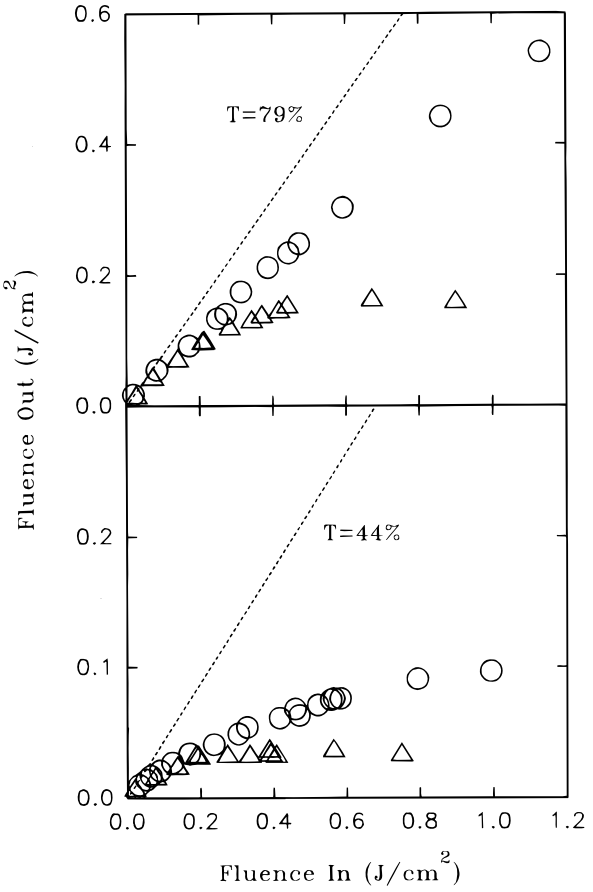

Figure 11. Optical limiting results of the methano-C_{60} derivative **I** in PMMA films (~0.4 mm thickness) with linear transmittances of 79 and 44% at 532 nm (○). The results of the compound in toluene solutions with the same linear transmittances (△) are also shown for comparison.

films. Shown in Figure 11 are the optical limiting responses of the films with linear transmittances of 79% and 44% at 532 nm, which are compared with the results of the C_{60} derivative **I** in toluene solutions of the same linear transmittances. Although both films show optical limiting, the responses are much weaker in the films than in the corresponding solutions. For the films, the output fluences show no plateau even at input fluences of 1 J/cm^2 and higher (Figure 11).

Discussion

The functionalized fullerene molecules studied here represent different classes of C_{60} derivatives. They have different molecular structures, with significantly different functional groups on the fullerene cage. However, the photophysical properties of the derivatives, though noticeably different from those of the parent C_{60}, are rather similar. Qualitatively, the overall increases in molar absorptivities from C_{60} to the C_{60} derivatives are nearly the same. Because the absorptivity increases may be attributed to a reduction in molecular symmetry due to the functionalization of the C_{60} cage, the results indicate that the electronic transitions in the C_{60} derivatives reported here and those already reported in the literature are likely dictated by the electronic structures of the functionalized fullerene moiety. In addition, a common feature in the absorption spectra of the different C_{60} derivatives is the weak 0−0 transition band near 695 nm.[27−32] It may be concluded qualitatively that the lowest electronic transitions in different classes of C_{60} derivatives have similar energies and transition probabilities.

In a more quantitative comparison, the absorption spectrum of the C_{60} derivative **VI** is somewhat different from those of methano-C_{60} derivatives, but rather similar to those of pyrrolidino-C_{60} derivatives (Figure 3). The similarity may have something to do with the fact that in the C_{60} derivative **VI** and pyrrolidino-C_{60} derivatives the fullerene cage is functionalized through the [6,6]-junction with a five-member ring, though the derivative **VI** has a cage-oxygen linkage. On the other hand, the cage functionalization in the amino-C_{60} derivative **VII** is also 1,2-addition through the closed [6,6]-ring junction, but its absorption spectrum is noticeably different from the spectra of other classes of C_{60} derivatives. The most obvious difference in the spectrum of the amino-C_{60} derivative **VII** is the absence of a well-resolved peak at 400 − 450 nm, which is well-known as a characteristic feature in the spectra of methano-C_{60} and pyrrolidino-C_{60} derivatives.[27−32] Although the amino-C_{60} derivative **VII** consists of a six-membered ring instead of the five-membered ring in the C_{60} derivative **VI** and pyrrolidino-C_{60} derivatives and the three-membered ring in methano-C_{60} derivatives, its different absorption spectrum is probably due primarily to the cage-nitrogen linkages because the spectra of the C_{60} derivatives that consist of a cyclohexane ring are similar to those of methano-C_{60} and pyrrolidino-C_{60} derivatives.[27a] In a separate note, because the absorption spectrum of the amino-C_{60} derivative has only limited structures, it seems no surprise that upon attaching C_{60} cages to polyethylenimine, the absorption spectrum of the C_{60}-aminopolymer becomes a structureless curve due to spectral broadening effects associated with polymeric structures.[40]

The fluorescence properties of the C_{60} derivatives are apparently insensitive to the molecular structural differences in the derivatives. The fluorescence spectra of the different classes of C_{60} derivatives are rather similar, with only minor changes in the relative intensities of the vibrational bands (Figures 3 and 4). For all the derivatives, the 0−0 bands in the fluorescence spectra correspond well to the 0−0 bands in the absorption spectra (Figure 3). The mirror-image relationship between the 0−0 absorption and fluorescence bands suggests that the lowest-energy absorption and emission are associated with the same excited singlet state for the C_{60} derivatives in room-temperature solution. It may be argued that the lowest-energy electronic

transitions in C_{60} derivatives are dictated by the functionalized C_{60} cage and are little affected by the functional groups in different classes of C_{60} derivatives.

The observed absorption spectra of the different classes of C_{60} derivatives suggest that the different cage functionalizations have more significant effects on the higher-energy electronic transitions. The results may be used as evidence for the argument that the observed absorptions in the visible region (440−650 nm) are due in large part to contributions of electronic transitions other than the transition to the lowest excited singlet state. The absorption contributions in the region should therefore not be included in the calculation of fluorescence transition probabilities in terms of the Strickler−Berg equation.[41] With the assumption that the absorption due to the lowest electronic transition may be estimated by the mirror image of the observed fluorescence spectrum, the calculated fluorescence radiative rate constants $k_{F,c}$ of the C_{60} derivatives are somewhat smaller than the experimental $k_{F,e}$ values obtained from the fluorescence quantum yield and lifetime results.[30] For C_{60}, it has been shown[5,6,42,43] that a similar estimate of the lowest-lying electronic transition probability by using the assumed fluorescence-absorption mirror image relationship results in a $k_{F,c}$ value somewhat larger than the $k_{F,e}$ value. Nevertheless, because the calculation of $k_{F,c}$ values is sensitive to the rough assumption of the mirror-image relationship between fluorescence and absorption and also to other approximations associated with the Strickler−Berg equation,[41] some discrepancies between $k_{F,c}$ and $k_{F,e}$ values might be expected. Thus, the mirror-image assumption, though a rough approximation, still provides a qualitative measurement for the portion in the observed absorption spectrum that is due to the transition to the lowest excited singlet state in C_{60} and C_{60} derivatives.

The fluorescence quantum yields and lifetimes of the different C_{60} derivatives are all very similar. The results further support the conclusion that the electronic transitions in C_{60} derivatives are dictated by the electronic structures of the functionalized fullerene moiety and are little affected by the functional groups in different classes of C_{60} derivatives. From C_{60} to the C_{60} derivatives, both fluorescence quantum yields and lifetimes increase. However, the increases in quantum yields are larger than those in lifetimes, corresponding to larger fluorescence radiative rate constants of the C_{60} derivatives than that of C_{60}. The results are consistent with higher molar absorptivities for the 0−0 transitions in the C_{60} derivatives. From the comparison of the C_{60} derivatives, it is obvious that the difference in the fluorescence properties is much less significant among different classes of C_{60} derivatives than between the derivatives and C_{60}.

Similar to the parent C_{60}, the C_{60} derivatives exhibit significant optical limiting responses toward a nanosecond pulsed laser at 532 nm. The optical limiting properties of C_{60} have been explained in terms of a reverse saturable absorption mechanism.[10] A five-level model (Scheme 1) has been used to describe the reverse saturable absorption in fullerenes and organic dyes. As the incident light transmits through the sample with a pathlength of L, the photon flux i (photons cm^{-2} s^{-1}) changes with the distance x in a nonlinear fashion due to significant excited-state absorptions.

$$di/dx = -\sigma_G N_G i - \sigma_S N_S i - \sigma_T N_T i \qquad (2)$$

where σ denotes absorption cross sections (cm^2) and the subscripts (G, S, and T) indicate the corresponding electronic states as shown in Scheme 1, and N represents the molecular populations in the different states, which are time dependent.

SCHEME 1

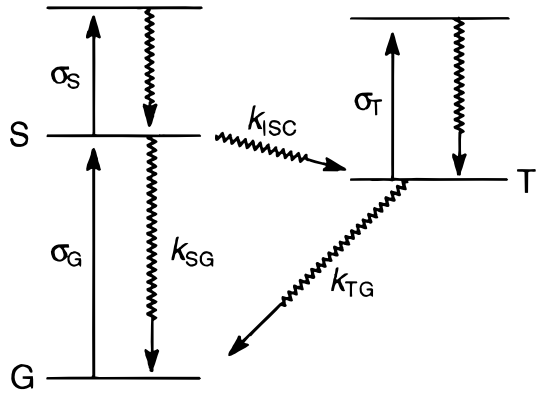

By assuming that the populations in the upper excited states are negligible,

$$dN_S/dt = \sigma_G N_G i - (k_{SG} + k_{ISC})N_S \qquad (3)$$

$$dN_T/dt = k_{ISC} N_S - k_{TG} N_T \qquad (4)$$

An expression for N_G is not necessary because of the relationship $N_G = N - (N_S + N_T)$, where N is the total molecular population. Reverse saturable absorption occurs when the excited-state cross sections are larger than the ground-state cross section, $\sigma_{EFF}/\sigma_G > 1$, where σ_{EFF} includes a weighted average of σ_S and σ_T.[44] This situation is certainly the case for C_{60}, with both σ_S and σ_T significantly larger than σ_G at 532 nm.[7,8,10] For modeling the optical limiting properties of C_{60} in toluene solution, McLean et al.[10] have used numerical integrations to solve the differential eqs 2−4 of the five-level model for reverse saturable absorption (Scheme 1). The results show that the optical limiting of C_{60} follows the five-level model with incident light fluences at 532 nm up to ~1 J/cm^2, and that for the 8-ns pulsed laser, the optical limiting response is due predominantly to the strong absorption of the excited triplet state of C_{60}.

The optical limiting properties of the C_{60} derivatives may similarly be explained in terms of the reverse saturable absorption mechanism (Scheme 1). Because photoexcited methano- and pyrrolidino-C_{60} derivatives generate singlet molecular oxygen as efficiently as C_{60} in solution,[45] their intersystem crossing yields should be close to unity like C_{60}. For other C_{60} derivatives, available experimental results also show large intersystem crossing yields.[27a,46] Thus, the optical limiting responses of the C_{60} derivatives under consideration may again be attributed predominantly to the stronger excited triplet-state absorption than the ground-state absorption, $\sigma_T/\sigma_G > 1$. However, what is interesting is that the optical limiting responses of different classes of C_{60} derivatives are not only nearly identical among themselves but also essentially the same as those of C_{60} in room-temperature solutions (Figures 7 and 9). With the great similarities among the excited singlet-state properties of different classes of C_{60} derivatives, their excited triplet-state properties may also be expected to be very similar. Such similarities may explain the same optical limiting responses of different classes of C_{60} derivatives.

The transient absorption properties of some C_{60} derivatives have been reported.[27a,d,g,28] In particular, it has been shown that the triplet−triplet molar absorptivities of the C_{60} derivative **IV** are smaller than those of C_{60}.[28] Such a decrease in the excited-state absorptivities appears to be a general phenomenon associated with the mono-functionalization of the C_{60} cage.[28] Even with the characteristic blue-shift in the triplet−triplet absorption

spectrum from C_{60} to the derivatives such as **IV**,[28,47] the triplet-state absorption cross section at 532 nm is still smaller in the derivative than in C_{60}. On the other hand, the ground-state absorption cross section of the C_{60} derivative is somewhat higher than that of C_{60}. Thus, $(\sigma_T/\sigma_G)_{Derivative} < (\sigma_T/\sigma_G)_{C60}$. The fact that the optical limiting responses of C_{60} derivatives and C_{60} are essentially the same suggests other contributions beyond the nonlinear absorption associated with the (σ_T/σ_G) factor. It is a possibility that the contribution due to the excited singlet-state absorption is more significant in the C_{60} derivatives than in C_{60}. The fluorescence lifetimes of the derivatives are longer than that of C_{60} (Table 1). As a result, the longer-lived singlet−singlet transient absorption in the C_{60} derivatives may contribute more to the limiting of the nanosecond laser pulse. However, in view of the significantly different optical limiting responses for the C_{60} derivative **I** in solution versus in PMMA film (Figure 11), optical limiting contributions from mechanisms other than the reverse saturable absorption may not be ruled out completely. Similarly, different optical limiting responses for C_{60} in solution versus in PMMA matrix have been reported.[21] It seems difficult to explain the results within the context of the reverse saturable absorption mechanism because, according to laser flash photolysis measurements, the triplet transient absorption spectra of C_{60} in solution and in PMMA film are quite similar.[48] For C_{60}, there is a possibility that the fullerene molecules form aggregates in the polymer matrix due to solubility characteristics. The interactions between excited singlet-state and ground-state fullerene molecules in the aggregates may compete with intersystem crossing,[49] resulting in reduced excited triplet-state population and thus weaker optical limiting responses. However, the aggregation problem should be less significant in the C_{60} derivative because of its much improved solubilities in common organic solvents, from which the polymer films can be prepared. Thus, the observed significant difference between the optical limiting responses of the C_{60} derivative in solution and in PMMA film may suggest more complicated mechanisms, at least for the optical limiting behavior in the films. Further investigations are required in this regard.

Acknowledgment. We thank Bing Liu, Xian-Fu Zhang, and Christopher Bunker for experimental assistance. Financial support from the National Science Foundation (CHE-9320558 and CHE-9727506) is gratefully acknowledged. The research assistantship for Bin Ma was provided in part by the Department of Energy through DOE/EPSCoR cooperative agreement DE-FG02-91ER75666. Dwella Moton was a participant in the Summer Undergraduate Research Program sponsored jointly by the National Science Foundation (CHE-9100387 and CHE-9619573) and by Clemson University.

References and Notes

(1) Foote, C. S. in *Topics in Current Chemistry: Electron-Transfer I*; Mattay, J. Ed.; Springer-Verlag: Berlin, 1994; p 347.

(2) Sun, Y.-P. In *Molecular and Supramolecular Photochemistry, Vol. 1*; Ramamurthy, V., Schanze, K. S. Eds., Marcel Dekker: New York, 1997; p 325.

(3) (a) Ajie, H.; Alvarez, M. M.; Anz, S. J.; Beck, R. D.; Diederich, F.; Fostiropoulos, K.; Huffman, D. R.; Kratschmer, W.; Rubin, Y.; Schriver, K. E.; Sensharma, D.; Whetten, R. L. *J. Phys. Chem.* **1990**, *94*, 8630. (b) Taylor, R.; Hare, J. P.; Abdulsada, A.; Kroto, H. W. *J. Chem. Soc. Chem. Commun.* **1990**, 1423.

(4) Arbogast, J. W.; Darmanyan, A. P.; Foote, C. S.; Rubin, Y.; Diederich, F. N.; Alvarez, M. M.; Whetten, R. B. *J. Phys. Chem.* **1991**, *95*, 11.

(5) Sun, Y.-P.; Wang, P.; Hamilton, N. B. *J. Am. Chem. Soc.* **1993**, *115*, 6378.

(6) Ma, B.; Sun, Y.-P. *J. Chem. Soc., Perkin Trans. 2* **1996**, 2157.

(7) Ebbeson, T. W.; Tanigaki, K.; Sadanori, K. *Chem. Phys. Lett.* **1991**, *181*, 501.

(8) Lee, M.; Song, O.-K.; Seo, J.-C.; Kim, D. *Chem. Phys. Lett*. **1992**, *196*, 325.

(9) Tutt, L. W.; Kost, A. *Nature* **1992**, *356*, 225.

(10) McLean, D. G.; Sutherland, R. L.; Brant, M. C.; Brandelik, D. M. *Opt. Lett.* **1993**, *18*, 858.

(11) (a) Mclean, D. G.; Brant, M. C. *Proc. SPIE-Int. Soc. Opt. Eng*. **1993**, *1856*, 162. (b) Brant, M. C.; Brandelik, D. M.; Mclean, D. G.; Sutherland, R. L.; Fleitz, P. A. *Mol. Cryst. Liq. Cryst*. **1994**, *256*, 807.

(12) (a) Joshi, M. P.; Mishra, S. R.; Rawat, H. S.; Mehendale, S. C.; Rustagi, K. C. *Appl. Phys. Lett.* **1993**, *62*, 1763. (b) Justus, B. L.; Kafafi, Z. H.; Huston, L. *Opt. Lett*. **1993**, *18*, 1603. (c) Lindle, J. R.; Pong, R. G. S.; Bartoli, F. J.; Kafafi, Z. H. *Phys. Rev. B* **1993**, *48*, 9447. (d) Wray, J. E.; Liu, K. C.; Chen, C. H.; Garett, W. R.; Payne, M. G.; Goedert, R.; Templeton, D. *Appl. Phys. Lett*. **1994**, *64*, 2785. (e) Kost, A.; Jensen, J. E.; Klein, M. B.; Marvin, B.; McCahon, S. W.; Haeri, M. B.; Ehritz, M. E. *Proc. SPIE-Int. Soc. Opt. Eng.* **1994**, *2229*, 78. (f) Heflin, J. R.; Wang, S.; Marciu, D.; Freeland, J. W.; Jenkins, B. *Polym. Prepr*. **1994**, *35*, 238. (g) Li, C.; Si, J.; Yang, M.; Wang, R.; Zhang, L. *Phys. Rev. A* **1995**, *51*, 569. (h) Koudoumas, E.; Ruth, A. A.; Couris, S.; Leach, S. *Mol. Phys*. **1996**, *88*, 125. (i) Golovlev, V. V.; Garrett, W. R.; Chen, C. H. *J. Opt. Soc. Am. B.* **1996**, *13*, 2801. (j) Guha, S.; Roberts, W. T.; Ahn, B. H. *Appl. Phys. Lett.* **1996**, *68*, 3686.

(13) (a) Mishra, S. R.; Rawat, H. S.; Joshi, M. P.; Mehendale, S. C. *Appl. Phys. A: Mater. Sci. Process*. **1996**, *A63*, 223. (b) Issac, R. C.; Bindhu, C. V.; Harilal, S. S.; Varier, G. K.; Nampoori, V. P. N.; Vallabhan, C. P. G. *Mod. Phys. Lett. B* **1996**, *10*, 61. (c) Hood, P. J.; Edmonds, B. P.; Mclean, D. G.; Brandelik, D. M. *Proc. SPIE-Int. Soc. Opt. Eng*. **1994**, *2229*, 91. (d) Nashold, K. M.; Walter, D. P. *J. Opt. Soc. Am. B* **1995**, *12*, 1228.

(14) (a) Henari, F.; Callaghan, J.; Stiel, H.; Blau, W.; Cardin, D. J. *Chem. Phys. Lett*. **1992**, *199*, 144. (b) Heflin, J. R.; Marciu, D.; Figura, C.; Wang, S.; Burbank, P.; Stevenson, S.; Dorn, H. C.; Withers, J. C. *Proc. SPIE-Int. Soc. Opt. Eng.* **1996**, *2854*, 162. (c) Couris, S.; Koudoumas, E.; Ruth, A. A.; Leach, S. *J. Phys. B. At. Mol. Opt. Phys.* **1995**, *28*, 4537.

(15) (a) Li, C.; Zhang, L.; Wang, R.; Song, Y.; Wang, Y. *J. Opt. Soc. Am. B* **1994**, *11*, 1356. (b) Li, C.; Yang, M.; Guo, F.; Wang, Y.; Tada, K. *Int. J. Nonlinear Opt. Phys.* **1993**, *2*, 551.

(16) (a) Brandelik, D. M.; Frock, L. R.; Brant, C. M.; Mclean, D. G.; Sutherland, R. L. *Proc. SPIE-Int. Soc. Opt. Eng.* **1995**, *2530*, 188. (b) Heflin, J. R.; Wang, S.; Marciu, D.; Figura, C.; Yordanov, R.; *Proc. SPIE-Int. Soc. Opt. Eng.* **1995**, *2530*, 176. (c) Cha, M.; Sariciftci, N. S.; Heeger, A. J.; Hummelen, J. C.; Wudl, F. *Appl. Phys. Lett.* **1995**, *67*, 3850.

(17) (a) Gvishi, R.; Bhawalkar, J. D.; Kumar, N. D.; Ruland, G.; Narang, U.; Prasad, P. N. *Chem. Mater*. **1995**, *7*, 2199. (b) Prasad, P. N.; Gvishi, G. R.; Kumar, N. D.; Bhawalkar, J. D.; Narang, U. *Proc. SPIE-Int. Soc. Opt. Eng*. **1995**, *2530*, 128.

(18) (a) Maggini, M.; Scorrano, G.; Prato, M.; Brusatin, G.; Innocenzi, P.; Guglielmi, M.; Renier, A.; Signorini, R.; Meneghetti, M.; Bozio, R. *Adv. Mater*. **1995**, *7*, 404. (b) Maggini, M.; Scorrano, G.; Prato, M.; Brusatin, G.; Gugliemi, M.; Meneghetti, M.; Bozio, R. *Proc. Electochem. Soc*. **1995**, *95*−*10*, 84. (c) Signorini, R.; Zerbetto, M.; Meneghetti, M.; Bozio, R.; Maggini, M.; De Faveri, C.; Prato, M.; Scorrano, G. *J. Chem. Soc. Chem. Commun.* **1996**, 1891. (d) Signori, R.; Zerbetto, M.; Meneghetti, M.; Bozio, R.; Maggini, M.; Scorrano, G.; Prato, M.; Brusatin, G.; Menegazzo, E.; Guglielmi, M. *Proc. SPIE-Int. Soc. Opt. Eng.* **1996**, *2854*, 130.

(19) (a) McBranch, D. W.; Mattes, B. R.; Koskelo, A. C.; Robinson, J. M.; Love, A. C. *Proc. SPIE-Int. Soc. Opt. Eng.* **1994**, *2284*, 15. (b) Brunel, M.; Canva, M.; Brun, A.; Chaput, F.; Malier, L.; Boilot, J. P. *Mater. Res. Soc. Symp. Proc*. **1995**, *374*, 281. (c) McBranch, D.; Smilowitz, L.; Klimov, V.; Koskelo, A.; Robinson, J. M.; Mattes, B. R.; Hummelen, J. C.; Wudl, F.; Withers, J. C.; Borrelli, N. F. *Proc. SPIE-Int. Soc. Opt. Eng.* **1995**, *2530*, 196. (d) McBranch, D.; Klimov, V.; Smilowitz, L.; Grigorova, M.; Robinson, J. M.; Koskelo, A.; Mattes, B. R.; Wang, H.; Wudl, F. *Proc. SPIE-Int. Soc. Opt. Eng*. **1996**, *2854*, 140.

(20) Smilowitz, L.; McBranch, D.; Klimov, V.; Robinson, J. M.; Koskelo, A.; Grigorova, M.; Mattes, B. R.; Wang, H.; Wudl, F. *Opt. Lett.* **1996**, *21*, 922.

(21) Kost, A.; Tutt, L.; Klein, M. B.; Dougherty, T. K.; Elias, W. E. *Opt. Lett*. **1993**, *18*, 334.

(22) Kojima, Y.; Matsuoka, T.; Takahashi, H.; Kurauchi, T. *Macromolecules* **1995**, *28*, 8868.

(23) Sun, Y.-P.; Riggs, J. E. *J. Chem. Soc., Faraday Trans.* **1997**, *93*, 1965.

(24) Sun, Y.-P.; Riggs, J. E. *Chem. Mater*. **1997**, *9*, 1268.

(25) Hirsch, A. *The Chemistry of Fullerenes*; Thieme: Stuttgart, 1994.

(26) Diederich, F.; Thilgen, C. *Science* **1996**, *271*, 317.

(27) (a) Anderson, J. L.; An, Y.-Z.; Rubin, Y.; Foote, C. S. *J. Am. Chem. Soc.* **1994**, *116*, 9763. (b) Lin, S.-K.; Shiu, L.-L.; Chien, K. M.; Luh, T.-Y.; Lin, T.-I. *J. Phys. Chem.* **1995**, *99*, 105. (c) Williams, R. M.; Zwier, J. M.; Verhoeven, J. W. *J. Am. Chem. Soc.* **1995**, *117*, 4093. (d) Bensasson, R. V.; Bienvue, E.; Janot, J.-M.; Leach, S.; Seta, P.; Schuster, D. I.; Wilson, S. R.; Zhao, H. *Chem. Phys. Lett*. **1995**, *245*, 566. (e) Brezova, V.; Stasko,

A.; Rapta, P.; Domschke, G.; Bartl, A.; Dunsch, L. *J. Phys. Chem*. **1995**, *99*, 16234. (f) Bennati, M.; Grupp, A.; Mehring, M.; Belik, P.; Gugel, A.; Mullen, K. *Chem. Phys. Lett*. **1995**, *240*, 622. (g) Nakamura, Y.; Minowa, T.; Hayashida, Y.; Tobita, S.; Shizuka, H.; Nishimura, J. *J. Chem. Soc., Faraday Trans*. **1996**, *92*, 377. (h) Hamano, T.; Okuda, K.; Mashino, T.; Hirobe, M.; Arakane, K.; Ryu, A.; Mashiko, S.; Nagano, T. *J. Chem. Soc. Chem. Commun*. **1997**, 21. (i) Baran, P. S.; Monaco, R. R.; Khan, A. U.; Schuster, D. I.; Wilson, S. R. *J. Am. Chem. Soc*. **1997**, *119*, 8363.

(28) (a) Guldi, D. M.; Hungerbuehler, H.; Asmus, K.-D. *J. Phys. Chem*. **1995**, *99*, 9380. (b) Guldi, D. M.; Asmus, K.-D. *J. Phys. Chem. A* **1997**, *101*, 1472.

(29) (a) Guldi, D. M.; Hungerbuhler, H.; Asmus, K.-D. *J. Phys. Chem*. **1995**, *99*, 13487. (b) Guldi, D. M.; Hungerbuhler, H.; Asmus, K.-D. *J. Phys. Chem. A*. **1997**, *101*, 1783.

(30) Ma, B.; Bunker, C. E.; Guduru, R.; Gord, J. R.; Sun, Y.-P. *J. Phys. Chem. A* **1997**, *101*, 5626.

(31) (a) Isaacs, L.; Diederich, F. *Helv. Chim. Acta* **1993**, *76*, 1231. (b) Isaacs, L.; Diederich, F. *Helv. Chim. Acta* **1993**, *76*, 2454.

(32) Maggini, M.; Scorrano, G.; Prato, M. *J. Am. Chem. Soc*. **1993**, *115*, 9798.

(33) Wang, Y.; Cao, J.; Schuster, D. I.; Wilson, S. R. *Tetrahedron Lett*. **1995**, *36*, 6843.

(34) Sheehan, J. C.; Preston, J.; Cruickshank, P. A. *J. Am. Chem. Soc*. **1965**, *87*, 2492.

(35) Bingel, C. *Chem. Ber*. **1993**, *126*, 1957.

(36) (a) Hirsch, A.; Lamparth, I.; Karfunkel, H. R. *Angew. Chem., Int. Ed. Engl*. **1994**, *33*, 437. (b) Lamparth, I.; Hirsch, A. *J. Chem. Soc. Chem. Commun*. **1994**, 1727.

(37) Lawson, G. E.; Kitaygorodskiy, A.; Ma, B.; Bunker, C. E.; Sun, Y.-P. *J. Chem. Soc. Chem. Commun*. **1995**, 2225.

(38) Kampe, K.-D.; Egger, N.; Vogel, M. *Angew. Chem., Int. Ed. Engl*. **1993**, *32*, 1174.

(39) Parker, C. A. *Photoluminescence of Solutions*; Elsevier: Amsterdam, 1968.

(40) Sun, Y.-P.; Bunker, C. E.; Liu, B. *Chem. Phys. Lett*. **1997**, *272*, 25.

(41) Strickler, S. J.; Berg, R. A. *J. Chem. Phys*. **1962**, *37*, 814.

(42) Sension, R. J.; Phillips, C. M.; Szarka, A. Z.; Romanow, W. J.; McGhie, A. R.; McCauley, J. P., Jr.; Smith, A. B., III.; Hochstrasser, R. M. *J. Phys. Chem*. **1991**, *69*, 6075.

(43) Kim, D.; Lee, M.; Suh, Y. D.; Kim, S. K. *J. Am. Chem. Soc*. **1992**, *114*, 4429.

(44) Perry, J. W.; Mansour, K.; Lee, I.-Y. S.; Wu, X.-L.; Bedworth, P. V.; Chen, C.-T.; Ng, D.; Marder, S. R.; Miles, P.; Wada, T.; Tian, M.; Sasabe, H. *Science* **1996**, *273*, 1533.

(45) Foote, C. S. *Am. Chem. Soc. Symp. Ser. 616 (Light Activated Pest Control)*, **1995**, 17.

(46) Sun, Y.-P.; Bunker, C. E.; Lawson, G. E.; Wang, N.; Dabestani, R., unpublished results.

(47) Weisman, R. B.; Ausman, K. D.; Benedetto, A.; Samuels, D. *Proc. SPIE-Int. Soc. Opt. Eng*. **1997**, *3142*, 260.

(48) Gevaert, M.; Kamat, P. V. *J. Phys. Chem*. **1992**, *96*, 9883.

(49) (a) Sun, Y.-P.; Bunker, C. E. *Chem. Mater*. **1994**, *6*, 578. (b) Ma, B.; Sun, Y.-P., manuscript in preparation.